Environment International 207 (2026) 110022

Contents lists available at ScienceDirect

Environment International

journal homepage: www.elsevier.com/locate/envint

Full length article

Characterizing adaptive capacity for the future heat-related cardiovascular morbidity burden in U.S. Metropolitan areas

Wei-Lun Tsai [a,*], E.Melissa Mcinroe [b], Anna M. Jalowska [a], Corinna Y. Keeler [a], Stephanie E. Cleland [c], Cassandra R. O'Lenick [d], Tanya L. Spero [a], Alexandra Schneider [e], Ana G. Rappold [a]

[a] Office of Research and Development, U.S. Environmental Protection Agency, Research Triangle Park, NC, United States
[b] ORAU National Student Services Contractor at Office of Research and Development, U.S. Environmental Protection Agency, Research Triangle Park, NC, United States
[c] Faculty of Health Sciences, Simon Fraser University, B.C., Canada
[d] Center for Environmental Medicine, Asthma, and Lung Biology, University of North Carolina at Chapel-Hill, Chapel-Hill, NC, United States
[e] Institute of Epidemiology, Helmholtz Zentrum München, Munich, Germany

ARTICLE INFO

Keywords:
Extreme heat
CVD
Temperature projection
Health burden
Adaptive capacity
Medicare
LOCA

ABSTRACT

Exposure to excess heat is linked to increased risks of cardiovascular diseases (CVD). As temperatures increase globally, it is crucial to examine the potential increase in excess heat-related CVD (xHEAT-CVD) burden to inform strategies for adaptation. This study aimed to identify the contextual factors associated with future xHEAT-CVD burden among older adults across eighty U.S. metropolitan statistical areas (MSAs).

The MSA-specific xHEAT-CVD risk for adults ≥ 65 years was estimated using hospitalization and temperature data from 2000 to 2017, with excess heat defined as temperatures above the minimum hospitalization percentile (T_{MHP}). Future xHEAT-CVD hospitalizations were estimated using temperature projections for 2025–2054, 2045–2074, and 2070–2099 under three climate scenarios. Area-level variables were used to identify demographic and economic status, health, environment, and infrastructure contexts and derive Urban Heat Health Risk (UHHR) scores using confirmatory factor analysis. The associations between adaptive capacity (the UHHR scores) and future xHEAT-CVD burden were examined.

In 2070–2099 under the mildest scenario, 36 more days annually were projected to be ≥ T_{MHP}, and xHEAT-CVD burden was projected to increase by at least 20.4-fold. Lower adaptive capacity was associated with greater increases in future xHEAT-CVD burden, over 9-fold increase per 1-unit increase in UHHR score (9.1, 95 % Confidence Intervals: 2.8–15.4). The historical xHEAT-CVD burden (2000–2017) was largely driven by the health context, whereas environment played a more important role in the future.

Our findings suggest that drivers of the xHEAT-CVD burden may vary across time. Targeting the areas with the highest xHEAT-CVD burden at varying timeframes can help mitigate xHEAT-CVD burden more effectively.

1. Introduction

In the past two decades, approximately 490,000 deaths per year worldwide have been attributed to excess heat (Zhao et al., 2021), with greater impacts observed in urban areas (Madrigano et al., 2015). With the trajectory of temperature increases in projections under future emission scenarios (IPCC, 2023; Lee et al., 2021), it is crucial to understand the magnitude of health burden related to excess heat.

The health risk assessment framework used in the Intergovernmental Panel on Climate Change (IPCC) Sixth Assessment Report (AR6) is a function of hazard, exposure, and vulnerability (Estoque et al., 2023; IPCC, 2023). In this framework, hazard refers to severe or extreme events, including climatic phenomenon; exposure typically refers to the elements that are at risk of exposure to the hazard and is commonly expressed as land use or population-related characteristics; and vulnerability refers to the lack of capacity to adapt, cope, mitigate, or change responses from the hazard (Cheng et al., 2021; Li et al., 2022). Applying the IPCC health risk assessment framework to the case of excess heat-related health risks, excess heat constitutes the component of hazard, which may be perceived differently based on the affected

* Corresponding author.
E-mail address: tsai.wei-lun@epa.gov (W.-L. Tsai).

https://doi.org/10.1016/j.envint.2025.110022
Received 27 August 2025; Received in revised form 1 December 2025; Accepted 22 December 2025
Available online 23 December 2025

population's experience of heat intensity and biological susceptibility to adverse health impacts.

Urban areas are particularly affected, often experiencing amplified temperatures and health risks because of the urban heat island (UHI) effect (IPCC, 2023; Lee et al., 2021) and more communities at risk due to high population density. In the United States (US), urban areas are home to 82 % of adults aged 65 years old and over and 81 % of children younger than 5 years old (United Nations Statistics Division, 2025), two populations with demonstrated physiological susceptibility to heat. Studies have consistently reported that older adults have higher risks to excess heat burden due to physiological factors, such as reduced thermoregulatory responses and a higher prevalence of chronic conditions (Chen et al., 2024; García-León et al., 2024; Liu et al., 2022). Moreover, the greatest impacts of cardiovascular morbidity are observed in older adults residing in urban areas with high UHI intensity (Cleland et al., 2023). This emphasizes the need to understand how heat-related health burdens among older urban populations may change in the future. Therefore, older population residing in urban areas can be considered as the component of exposure in the case of excess heat-relate health risks.

In addition to disproportionately affecting at-risk populations, the compounding effects of demographic, economic, institutional, and environmental characteristics can further exacerbate heat-related health risks (Cheng et al., 2021; Conlon et al., 2020; Ebi et al., 2021). These characteristics can be considered aspects of vulnerability within the health risk framework, and a large body of research (Cheng et al., 2021; Conlon et al., 2020; Li et al., 2022) has identified numerous factors related to excess heat and human health which are frequently grouped based on context (Li et al., 2022) to help guide planning of potential interventions. The most common themes include demographic and economic factors, such as sex, income, educational attainment, housing structure, and economic hardship (Ellena et al., 2020; Gronlund, 2014; Ho et al., 2015; Rohat et al., 2019); health conditions, such as pre-existing chronic conditions and immunization status among children (Azhar et al., 2017; Ellena et al., 2020; Lin et al., 2009; Naughton et al., 2002; O'Lenick et al., 2019; Vandentorren et al., 2006; Wilhelmi and Hayden, 2010); environmental factors, such as air quality, greenspaces (Ellena et al., 2020; Gronlund et al., 2015; Harlan et al., 2006; Kalisa et al., 2018; Maragno et al., 2020; Reid et al., 2009); and infrastructure conditions, such as facilities in response to heat events (e.g., cooling centers, urgent care, hospitals), public transportation (Cutter et al., 2003; Ellena et al., 2020; Johnson et al., 2012; Nayak et al., 2018). Each of these themes (or "contexts") has been associated with elevated heat-related health risks.

Cardiovascular disease (CVD)-related hospitalizations have been strongly associated with extreme heat and carry significant economic burden (Cleland et al., 2023; Liu et al., 2022; Moghadamnia et al., 2017; Phung et al., 2016). This study leveraged nationwide individual-level data on CVD hospitalizations to investigate the magnitude of excess heat-related health burden across future scenarios and identify the contextual variables that shape those risks. We first modeled the future heat-related CVD burden based on current heat-related hospitalization risks, population growth rates, and future temperature projections. We then scored the urban heat health risk (UHHR) to characterize the relationships between projected future health burdens and current levels of adaptive capacity with respect to demographic/economic status, health, environment, and infrastructure under different scenarios. Finally, we examined the associations between UHHR scores and the projected changes in future heat-related CVD burden.

2. Materials and methods

2.1. Study population and cardiovascular outcome

This study focused on older adults who resided in urbanized areas in the contiguous U.S., a population with an increased risk of adverse health outcomes from excess heat exposure. We defined urbanized areas as metropolitan statistical areas (MSAs) in the contiguous U.S. with a total population of >= 500,000 based on the U.S. Census 2010 data (U.S. Census Bureau, 2020). Though heat-related risk of CVD burden may change over time, we were interested in understanding how CVD burden may change within the areas with higher susceptibility to excess heat-related CVD burden. Therefore, we focused on MSAs with increased heat-related relative risks of CVD hospitalizations identified by Cleland et al. (2023). Results based on all the MSAs (including those with decreased relative risks) are provided in Supplemental Results section. The increased relative risks here were modeled using the distributed lag non-linear model across 21 days (Cleland et al., 2023) and were not always associated with increased CVD hospitalization. Eighty MSAs met these criteria (Fig. 1), with a population density ranging from 20.2 people/km^2 in Boise, Idaho to around 2500 people/km^2 in Philadelphia, Pennsylvania. Detailed information on population, total land and water area, population density, and percent urban area based on the 2010 Census Urban and Rural Classification and Urban Area Criteria for the selected MSAs are provided in Supplemental Table 1. CVD hospitalizations were obtained from Medicare beneficiaries aged 65–114 within the 80 MSAs for 2000–2017 (defined as the historical period). Daily counts of CVD hospitalizations were first obtained at the ZIP Code Tabulation Area (ZCTA) level using the Medicare billing claims from short-stay, inpatient hospitalizations and then aggregated to the MSA level. Detailed information about the diagnosis codes for CVD-related hospitalizations (ICD-9: 390–438, ICD-10: I00-I69) used in this study are detailed in Cleland et al. (2023).

2.2. Temperature and population projections

Projected mean daily temperature from the Coupled Model Intercomparison Project Phase 5 (CMIP5; Sheffield et al., 2013) ensemble of global climate models (GCMs) was statistically downscaled to 1/16-degree latitude–longitude (~6 km) grid using Localized Constructed Analogs (LOCA; Pierce et al., 2014) and was obtained from the USGS Geo Data Portal (USGS Geo Data Portal, 2023). The CMIP5 projections are based on Representative Concentration Pathways (RCPs; van Vuuren et al., 2011), which are internationally recognized scenarios of future global greenhouse gas concentrations. This study used data from RCP4.5, a moderate emission scenario, and RCP8.5, a high emissions scenario, with global temperature increasing by 1.1–2.6 °C and 2.6–4.8 °C, respectively, by the year 2100 (IPCC, 2013). The LOCA data were available as an ensemble of 32 downscaled GCMs on monthly timescales and as individual downscaled GCMs on a daily timescale. The monthly ensemble values were too temporally coarse to use in this study. The daily data in this analysis were sourced from two downscaled GCMs: Community Earth System Model version 1 (a.k.a the fourth version of the Community Climate System Model; CESM-CCSM4; Gent et al., 2011) under RCP4.5 ("CC4-rcp45") and RCP8.5 ("CC4-rcp85") scenarios, and Geophysical Fluid Dynamics Laboratory Coupled Model v3 under RCP8.5 scenario (GCM-CM3; "GC3-rcp85"; Donner et al., 2001). In summary, the three climate scenarios for temperature projections used in this analysis were CC4-rcp45, CC4-rcp85, and GC3-rcp85. These GCMs varied in climatological skill, and based on mean and extreme statistics, none of these models were CMIP5 outliers; CESM-CCSM4 was ranked 3rd and GFDL-CM3 17th within the ensemble (Sanderson et al., 2017). These GCMs produced near-average biases in mean rainfall over the contiguous United States and reduced biases for eastern North America (Sheffield et al., 2013). The choice of the GCMs was driven by data evaluation based on other studies (e.g., Jalowska et al., 2025), which were validated against historical data in previous research (Spero et al., 2016; Nolte et al., 2021) and were used in the Fourth National Climate Assessment (Nolte et al., 2018). The data was subset to MSA boundaries, and daily maximum and minimum temperature were extracted for each MSA using the 'extract' function in the R 'raster' package (Hijmans, 2018). The mean daily temperature data for each MSA, for three periods: near- (2025–2054), mid- (2045–2074), and

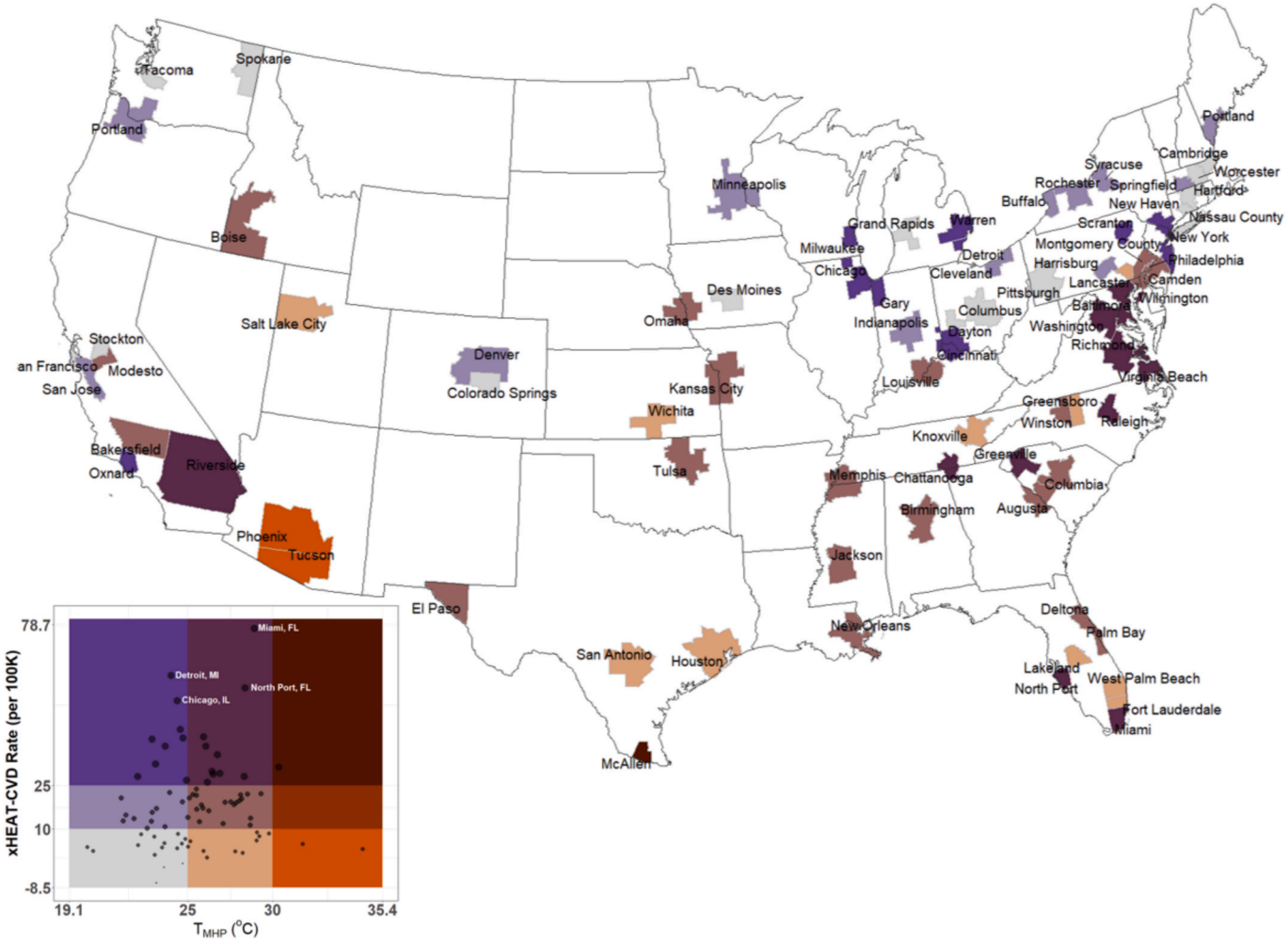

Fig. 1. Study areas (MSAs), temperature at the minimum hospitalization percentile (T_{MHP}), and excess heat-related CVD (xHEAT-CVD) burden rate at the historical period (2000–2017).

long-term (2070–2099) were derived using the average of the daily maximum and minimum temperature.

After CMIP5, a new set of scenarios called Shared Socioeconomic Pathways (SSPs), was developed to incorporate future societal development (O'Neill et al., 2014) as the foundation for CMIP6. The population projections by age at the county level under SSP2 ("middle of the road") and SSP5 ("fossil fuel development") for near- (2025–2054), mid- (2045–2074), and long- term (2070–2099) periods were obtained from the NASA's dataset (Hauer and Center for International Earth Science Information Network (CIESIN) at Columbia University, 2025). Subsequently, CMIP6 climate projections merged RCPs with SSPs. However, at the time of the study, LOCA2v1 data from CMIP6 (Pierce, 2021) lacked sufficient evaluation studies to support using the datasets here.

The unit of the analysis is MSA because the variability in outcome measure for future periods depends on three factors: spatial resolution of temperature in the future periods, historical incidence, and measure of risk. The latter two factors are based on the previous study by Cleland et al. (2023). The primary limiting factor is spatial resolution of temperature in the future periods, which typically downscaled from global climate model with a coarse resolution (e.g., 2°). In this analysis, we used a higher-resolution temperature data, LOCA, with a statistical downscaled data with a resolution of 1/16th degree, however, the resolution is still not adequate to capture the temperature variations at the ZCTA level. Supplemental Table 2 shows the variations of temperature above minimal hospitalization percentile (i.e., the temperatures used for the burden calculations) at the ZCTA level using CC4-rcp45 as an example for each MSA.

2.3. Area-level variables describing contexts for adaptive capacity

Area-level variables were selected based on two criteria that they have been previously shown as relevant modifiers of heat-health risks, and that data is available across the nation with negligible missingness. Variables used in this analysis were obtained from multiple sources and categorized into four contexts: demographic and economic status (DES), health (HLT), environment (ENV), and infrastructure (INF) (Supplemental Table 3). In this study, the *demographic and economic status* context characterizes demographic composition, financial capital, social cohesion and/or support, and stability of a place that may determine one's ability to regulate thermal comfort during extreme heat events; the *health* context represents the existing health issues that may affect the response to extreme heat exposure; the *environment* context describes the physical and climatic characteristics of the environments, and environmental hazards that may affect heat regulation and adaptation for a place in both historical and contemporary periods; and the *infrastructure* context characterizes local investments that may affect the preparedness to respond to extreme heat events. Around 20 variables were initially considered for each context (Supplemental Table 3), and a series of variable selections were conducted (see Section 2.4) to optimize the variables (Table 1) to generate the UHHR score for each context. All the variables were aggregated to the MSA level prior to analysis. Detailed descriptions and processing procedures of each variable are available in

Table 1
Data descriptions, years, sources, loadings from the confirmatory factor analysis for the selected variables in the demographic and economic (DES), health (HLT), environment (ENV), and infrastructure (INF) contexts used to describe adaptive capacity.

Context	Variable code	Description	Year(s)	Source(s)*	Loadings
DES	%MBSA	Percent population in management, business, science, and arts occupations	2015–2019	ACS	−0.89
	MedIncome	Median household income	2015–2019	ACS	−0.82
	EnergyBurden	Percentage of gross household income spent on energy costs in summer (June–September)	2018	Shen et al. (2023)	0.67
	%Mobile	Percent housing units that are mobile homes	2015–2019	ACS	0.63
	%EduLessHS	Percent population aged 25 and older with an education attainment less than high school or equivalent	2015–2019	ACS	0.62
	CSOrg	Number of civic and social organizations per 1,000 people	2003–2017	CVI	−0.61
	%NoHealthIns	Percent population without any health insurance	2015–2019	ACS	0.61
HLT	%AMI	Mean annual prevalence proportion of acute myocardial infarction	2019	CMS	0.90
	%Depression	Mean annual prevalence proportion of depression	2019	CMS	0.87
	%CKD	Mean annual prevalence proportion of chronic kidney diseases	2019	CMS	0.84
	%CHFChange	Change in mean prevalence proportion of congestive heart failure between 2011 and 2019	2011, 2019	CMS	−0.52
ENV	%Canopy	Mean canopy cover	2019	MRLC	−0.93
	Canopy/Impervious	Ratio of canopy and imperviousness	2019	MRLC	−0.74
	U/RCanopy	Ratio of canopy in urban versus rural areas	2019	MRLC, EnviroAtlas	0.64
	WildfireFreq	Annualized wildfire frequency	2000–2021	NRI	0.55
	DroughtFreq	Annualized drought frequency	1996–2019	NRI	0.54
	PM25	$PM_{2.5}$ in summer (June–September)	2000–2019	Atmospheric Composition Analysis Group, Washington University, St. Louis, Missouri, USA	−0.41
INF	ProxMedServ	Distance to the nearest medical facility (hospitals, urgent cares)	2024	HIFLD, Tiger	0.79
	%PoorPubTrans	Percent population in Census tracts with a Public Transit Performance Score below the national median score (i.e., 3.2)	2019	CVI	0.78
	% 15KMAwayMedServ	Percent population living within greater than 15 km away from a medical facility	2024	HIFLD, Tiger	0.69
	%PoorWalkability	Percent population in Census tracts with a Walkability Score below the national median score (i.e., 32)	2022	CVI	0.62
	CoolingPlaces	Averaged number of potential cooling places per sq. km	2010–2019	Census	−0.57

*ACS: U.S. Census American Community Survey 5-Year Estimate; Shen et al. (2023): dataset was obtained through personal communication; CVI: Climate Vulnerability Index; CMS: Center for Medicare and Medicaid Services; MRLC: Multi-Resolution Land Characteristics; EnviroAtlas: U.S. Environmental Protection Agency EnviroAtlas project; NRI: Federal Emergency Management Agency (FEMA) National Risk Index; HIFLD: Homeland Infrastructure Foundation-Level Data; Tiger: U.S. Census Bureau Topologically Integrated Geographic Encoding and Referencing system.

Supplemental Text.

2.4. Analytical approach

2.4.1. Main analysis

The analytical approach in this study included three steps (Fig. 2). Step 1 relied on MSA-specific exposure response functions and annual number of excess heat-related CVD hospitalizations per 100,000 beneficiaries (xHEAT-CVD burden rate) derived by Cleland et al. (2023) using NOAA daily temperature data from 2000 to 2017. In short, the distributed lag non-linear model across 21 days (lags 0–20) was used to model the exposure response association between temperature and CVD hospitalizations. A multivariate *meta*-regression then pooled relative risks across all MSAs to identify the temperature percentile at which the risk of CVD hospitalizations was minimized (hereafter, minimum hospitalization percentile [MHP]). MHP was derived using an approximate parametric bootstrap estimator (Tobías et al., 2017), a commonly used approach. The pooled estimates were then re-centered at the MHP (identified as the 92nd percentile) of the temperature distribution, and updated MSA-specific relative risks were derived using best linear unbiased prediction. This approach allowed each MSA to have the same MHP, but a different minimum hospitalization temperature (T_{MHP}) based on the distinct patterns of temperature in each MSA. Detailed information about the historical exposure data derivation and processing can be found in Cleland et al. (2023).

In Step 2, future xHEAT-CVD burden rates were derived using the MSA-specific exposure response functions from Step 1 and the daily temperature projections for years 2025–2099. Future daily xHEAT-CVD burden rates were then averaged for periods 2025–2054, 2045–2074, and 2070–2099 to represent near-, mid-, and long-term projections, respectively. Then, population projections for adults aged 65 and older for each MSA were obtained for the near-, mid-, and long-term under the SSP2 and SSP5 to correspond to RCP4.5 and RCP8.5, respectively. Changes in the population aged 65 and older were calculated using the population projections divided by the total population aged 65 and older based on the Decennial Census 2010 for each MSA. Lastly, future xHEAT-CVD burden rates were adjusted by multiplying the change in population aged 65 and older. Changes in xHEAT-CVD burden rates were then calculated by subtracting the historical xHEAT-CVD burden rates from the future xHEAT-CVD burden rates and dividing by the historical xHEAT-CVD burden rates for each GCMs under two RCPs paired with population projections in two SSPs at each term for each MSA. To summarize, the three climate scenarios for the xHEAT-CVD burden rates reported in this analysis are CC4-rcp45-ssp2, CC4-rcp85-ssp5, and GC3-rcp85-ssp5.

In Step 3, UHHR scores were generated based on the factor loadings of selected variables in each context using confirmatory factor analysis (CFA) using the 'lavaan' package in R (Rosseel, 2012). We used CFA because it enabled us to select a large set of indicator variables and group them by context based on the previously published literature (Cheng et al., 2021; Li et al., 2022) rather than use the universe of all indicators, which would be well-suited for principal component analysis (PCA). However, the two approaches are not fundamentally different, and sensitivity was done using PCA.

Prior to using CFA, we conducted variable selections. The evaluations occurred sequentially within each context with variable standardizations by removing variables with high correlations (>0.8), filtering out variables with a value less than 0.5 based on the Kaiser-Meyer-Olkin (KMO) test in the exploratory factor analysis, dropping the variables with a factor loading less than 0.5, and further removing

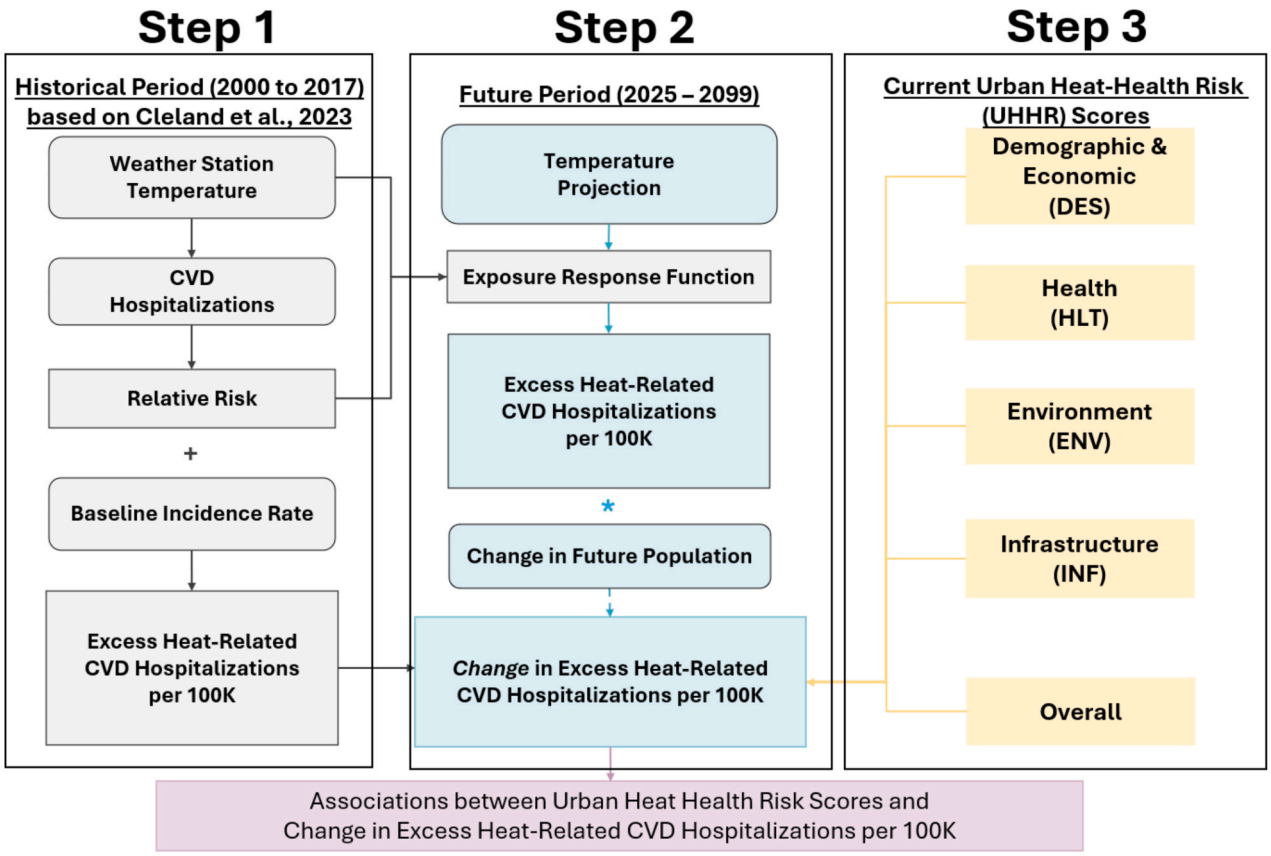

Fig. 2. Fig. 2. Analytical approach for this study.

variables with a loading less than 0.1 in the CFA. We used the variance standardization method for CFA, which fixes the variance of each factor to 1 to allow comparisons of factor loadings across the variables.

In addition to generating a UHHR score for each context and MSA, the final set of the variables in DES, HLT, ENV, and INF contexts (i.e., all the variables in Table 1) were combined to obtain loadings to create a latent variable for an overall UHHR score in each MSA.

Lastly, we examined how much the UHHR scores can characterize the relationships between future burdens and current levels of adaptive capacity with respect to demographic and economic, health, environment, and infrastructure contexts. The relationship between measures of current adaptive capacity and future projections of heat-health burden can provide better understanding about areas where adaptive capacity has to be improved. Linear regression was applied to model the associations between change in future xHEAT-CVD burden and the UHHR scores for the DES, HLT, ENV, and INF contexts, as well as the associations between change in future burden and the overall UHHR score. Part R-squared was used to measure the contribution of each context in the joint model. All the statistical analyses were conducted using RStudio with R version 4.4.1.

2.4.2. Sensitivity analysis

In addition to CFA, we also generated UHHR scores for the DES, HLT, ENV, and INF contexts, as well as an overall score, using PCA. We applied the set of variables in the first step of variable selections (i.e., variables without a correlation > 0.8) in the CFA analysis for PCA. In this sensitivity analysis, we only focused on the first component. Only variables with a percent contribution greater than the threshold calculated using 100 divided by the total number of variables within each context were retained. The scores of each context were derived for each MSA based on the eigenvectors. Similar to the CFA analysis, the final set of the variables in the DES, HLT, ENV, and INF contexts were combined to create an overall score for PCA. Linear regression and part R-squared were also applied to examine the associations between change in future burden and PCA scores of four contexts and overall, and the contribution of each context, respectively.

3. Results

3.1. Temperature and population projections and xHEAT-CVD burden rates

At the historical period, T_{MHP} ranged from 19.1 °C in Tacoma-Lakewood, Washington, to 35.4 °C in Phoenix-Mesa-Scottsdale, Arizona, with a mean ± standard deviation value of 25.6 ± 2.8 °C. For future projections on temperature and xHEAT-CVD burden (Table 2), it was expected that greater changes would be observed in the high emission/fossil fuel development scenario (RCP8.5/SSP5) compared to the changes observed in the moderate emission/middle of the road scenario (RCP4.5/SSP2), as well as by the long-term compared to the near-term. Between the two GCMs, greater changes were estimated by GFDL-CM3 (GC3) compared to CESM-CCSM4 (CC4). While the minimum and maximum values of future temperature percentile of T_{MHP} were observed by GC3-rcp85 and CC4-rcp45, respectively, the minimum and maximum values of number of days above T_{MHP} were observed by CC4-rcp45 and GC3-rcp85, respectively, across the near-, mid-, and long-term. Under the future temperature projection, T_{MHP} moved from the 92nd percentile at historical period to 80th ± 7 to 87th ± 5 for near-term, 73rd ± 7 to 84th ± 5 for mid-term, and 65th ± 8 to 83rd ± 6 for long-term ('pTile of T_{MHP}' in Table 2). In other words, while the mean number of days above T_{MHP} at the historical period was around 29 days for all the MSAs, the number of days above for T_{MHP} across the MSAs at the near-, mid-, and long-term ranged from 51 ± 19 to 76 ± 24, 60 ± 20 to 102 ± 27, and 65 ± 23 to 128 ± 28, respectively ('Days ≥ T_{MHP}' in

Table 2
Mean, standard deviation (sd), and range of: future temperature percentiles of the temperature at the minimum hospitalization percentile (92nd percentile) (pTile of T_{MHP}); number of days above T_{MHP} (Days $\geq T_{MHP}$); growth rate of the population aged 65 and older (Population Growth); excess heat-related cardiovascular disease hospitalizations per 100,000 beneficiaries per year (xHEAT-CVD burden rate); and changes in xHEAT-CVD burden rate (folds) between the historical and future periods (Change in xHEAT-CVD rate). Results are shown for the 80 Metropolitan Statistical Areas included in analysis. The historical period refers to 2000–2017, and near-, mid-, and long-term refers to 2025–2054, 2045–2074, and 2070–2099, respectively.

	pTile of T_{MHP}		**Days $\geq$ T_{MHP}**		Population Growth		**xHEAT-CVD rate**		**Change in xHEAT-CVD rate**	
80 MSAs	Mean (sd)	Range	Mean (sd)	Range	Mean (sd)	Range	Mean (sd)	Range	Mean (sd)	Range
Historical period	92.0 (0)	92.0–92.0	29.2 (0)	29.2–29.2	–	–	18.34 (15.71)	−8.45–78.72	–	–
CC4-rcp45-ssp2										
Near-term	86.5 (4.9)	73.7–97.9	51.3 (18.6)	8.5–100.0	2.13 (0.57)	1.19–4.30	111.66 (167.49)	−1.14–1182.91	5.44 (6.97)	−1.00–43.35
Mid-term	84.1 (5.4)	70.1–96.9	60.0 (20.4)	12.5–112.6	2.82 (1.13)	1.18–6.85	205.71 (314.78)	0.59–2172.26	11.47 (14.75)	−0.44–87.03
Long-term	82.6 (6.2)	66.9–96.4	65.4 (23.1)	14.3–124.6	3.74 (1.90)	1.15–10.28	349.52 (596.62)	1.35–4323.56	20.35 (27.90)	−0.44–180.64
CC4-rcp85-ssp5										
Near-term	84.2 (5.5)	69.5–97.0	59.5 (20.8)	11.3–115.0	2.36 (0.65)	1.29–4.79	184.35 (265.69)	0.66–1836.63	10.12 (13.00)	−0.72–89.89
Mid-term	79.5 (6.3)	62.4–93.6	76.5 (23.4)	24.0–140.2	3.43 (1.40)	1.38–8.40	479.61 (819.52)	−0.09–5885.10	28.95 (42.47)	−1.04–307.87
Long-term	73.6 (7.0)	54.2–87.8	98.0 (25.8)	45.7–169.6	5.03 (2.58)	1.48–13.92	1333.47 (2644.28)	0.02–19950.31	84.61 (138.17)	−0.99–950.00
GC3-rcp85-ssp5										
Near-term	79.8 (6.5)	62.9–95.3	75.5 (24.4)	18.1–138.7	2.36 (0.65)	1.29–4.79	307.08 (592.75)	−1.24–4335.20	17.48 (25.87)	0.23–170.09
Mid-term	72.5 (7.2)	54.6–89.3	101.8 (26.5)	39.9–168.1	3.43 (1.40)	1.38–8.40	1027.44 (2232.60)	10.08–17284.31	63.44 (100.01)	2.21–613.64
Long-term	65.2 (7.7)	44.6–81.9	128.3 (28.4)	66.9–204.9	5.03 (2.58)	1.48–13.92	2952.84 (6761.63)	46.31–52489.23	192.25 (329.97)	18.23–1961.99

CC4-rcp45-ssp2: Community Climate System Model (CESM-CCSM4) under RCP 4.5 adjusting for population growth for aged 65 and older under SSP2-4.5.
CC4-rcp85-ssp5: Community Climate System Model (CESM-CCSM4) under RCP 8.5 adjusting for population growth for aged 65 and older under SSP5-8.5.
GC3-rcp85-ssp5: Geophysical Fluid Dynamics Laboratory Coupled Model (GCM-CM3) under RCP 8.5 adjusting for population growth for aged 65 and older under SSP5-8.5.

Table 2).

Mean values of population growth rates (fold increase) for aged 65 and older under SSP2 for the near-, mid-, and long-term were 2.1 ± 0.6, 2.8 ± 1.1, and 3.7 ± 1.9, respectively ('Population Growth' in Table 2). As expected, the population growth rates were generally higher under SSP5, with mean values of 2.4 ± 0.7, 3.4 ± 1.4, and 5.0 ± 2.6 for the near-, mid-, and long-term, respectively. The highest population growth rates for the population aged 65 and older were consistently projected to be in Raleigh, North Carolina, across all the terms under SSP2 (population growth rate for the near-, mid-, and long-term: 4.3, 6.9, and 10.3) and SSP5 (population growth rate for the near-, mid-, and long-term: 4.8, 8.4, and 14.0). Conversely, the lowest population growth rates were projected to be in Scranton–Wilkes-Barre–Hazleton, Pennsylvania, and Detroit-Dearborn-Livonia, Michigan, under both SSP2 (lowest population growth rate for the near-, mid-, and long-term: 1.19, 1.18, and 1.15) and SSP5 (lowest population growth rate for the near-, mid-, and long-term: 1.29, 1.38, and 1.48).

At the historical period, the xHEAT-CVD burden rates ranged from −8.5 to 78.7 hospitalizations per 100,000 beneficiaries per year, with a mean value of 18.3 ± 15.7. In the future periods, the minimum and maximum values of the xHEAT-CVD rate and change in xHEAT-CVD rate were projected by CC4-rcp45 and GC3-rcp85, respectively, across the near-, mid-, and long-term. For xHEAT-CVD burden rates, the projected mean values under the mildest scenario (CC4-rcp45-ssp2) were 111.7 ± 167.5, 205.7 ± 314.8, 349.5 ± 596.6 per 100,000 beneficiaries per year for the near-, mid-, and long-term, respectively ('xHEAT-CVD rate' in Table 2). The magnitudes of the burden were increasingly larger across the near-, mid-, and long-term when comparing the different emission/societal development scenarios (rcp45-ssp2 vs. rcp85-ssp5). The mean value was 1.7, 2.3, and 3.8 times higher for the near-, mid-, and long-term in the CC4-rcp85-ssp5 compared to CC4-rcp45-ssp2 scenario. Similar trends occurred when comparing different GCMs (CC4 versus GC3) under the same emission/societal development scenario (rcp85-ssp5). The mean values were 1.7, 2.1, and 2.2 times higher for the near-, mid-, and long-term in the GC3-rpc85-ssp5 compared to CC4-rpc85-ssp5 scenario.

For changes in xHEAT-CVD burden rates ('Change in xHEAT-CVD rate' in Table 2), the ranges of fold change in mean values under the mildest scenario were 5.4 ± 7.0, 11.5 ± 14.8, and 20.4 ± 27.9 for the near-, mid-, and long-term. Similar to xHEAT-CVD rate, when comparing CC4-rcp45-ssp2 versus CC4-rpc85-ssp5 across the future periods, the magnitude of changes increased by 1.9, 2.5, 4.2 times, respectively, for the near-, mid-, long-term. The magnitude of changes was also higher when comparing GC3-rcp85-ssp5 versus CC4-rcp85-ssp5, with multiplicative growth of 1.7, 2.2, and 2.3 for the near-, mid-, and long-term.

3.2. Urban heat health risk scores by context

Overall, based on the direction of CFA loadings, higher UHHR scores for all four contexts described lower adaptive capacity or heightened vulnerability. For the DES context, percent population in management, business, science, and arts occupations, median household income, and number of social and civic organization per 1000 people were selected with negative loadings, whereas energy burden during the summer months, percent housing that is mobile homes, percent population aged

25 and older without a high school diploma, and percent population without health insurance were selected with positive loadings. This indicates that areas that lack economic and social resources/support tended to have higher scores in the DES context.

For the HLT context, change in prevalence of congestive heart failure (2011–2019) was selected with a negative loading, and variables with positive loadings included mean prevalence of acute myocardial infarction, depression, and chronic kidney diseases. Therefore, high UHHR scores for the HLT context indicated higher and persistent concentrations of individuals with one or more chronic diseases.

For the ENV context, mean canopy cover, ratio of canopy and imperviousness, and $PM_{2.5}$ during summer months were selected with negative loadings, whereas ratio of canopy in urban versus rural areas, annualized wildfire, and drought frequency were selected with positive loadings. This means that areas with low canopy, high levels of air pollution, less rural canopy, and high frequency of wildfire and drought had higher scores in the ENV context.

For the INF context, the average number of potential cooling places per square kilometer was selected with a negative loading, and variables with positive loadings included distance to the nearest medical facility (hospitals and urgent care), percent population living greater than 15 km away from a medical facility, percent population in census tracts with a Public Transit Performance Score less than the national median score, and percent population in census tracts with a Walkability Score less than the national median score. As such, higher values in the INF context may indicate a lack of facilities and/or transportation network in response to emergency needs.

For the overall UHHR score that included all variables, the ranks of the scores were most consistent with the DES context (Fig. 3). The MSAs with high UHHR scores in the DES context tended to have higher scores in the HLT and INF contexts and lower scores in the ENV context.

3.3. Associations of urban heat health risk (UHHR) scores and change in future burden

The overall UHHR score was associated with larger changes in burden rates across the near-, mid-, long-term for all scenarios (Table 3). The associations for the overall UHHR scores were inconclusive for the historical period, as individual contexts were inconsistent in sign and magnitude. Under the CC4-rcp45-ssp2, a unit increase in overall UHHR score increased the xHEAT-CVD burden rates by factors of 2.4 [95 % Confidence Intervals: 0.9–4.0], 4.8 [1.4–8.1], and 9.1 [2.8–15.4] for the near-, mid-, and long-term, respectively; 95 % confidence intervals shown. The magnitudes of the projected burden increases were at least doubled for the corresponding terms under the CC4-rcp85-ssp5, with respective coefficients of 4.9 [2.1–7.8], 13.6 [4.0–23.1], and 35.1 [3.4–66.8]. The associations between overall UHHR scores and projected burden changes under GC3-rcp85-ssp5 were generally greater than those projected by the CC4-rcp45-ssp2 and rcp85-ssp5 but were only significant for the near-term.

The associations with the four contexts (Table 3) show that the DES and HLT scores were associated with an increased burden at the historical period, whereas the ENV and INF contexts were negatively associated with the historical burden. Overall, the UHHR scores across the four contexts were consistently associated with greater changes in burden rates for the future terms under all scenarios, with larger and more significant associations in the ENV context. For the ENV context, the respective multipliers for the near-, mid- and long-term were 1.9 [-0.1–3.9], 4.9 [0.7–9.1] and 9.0 [1.0–17.1] under CC4-rcp45-ssp2, 3.9 [0.3–7.6], 12.3 [0–24.6], and 37.5 [-3.2–78.2] under CC4-rcp85-ssp5, and 7.2 [-0.4–14.7], 30.1 [0.8–59.4], and 104.4 [7.5–201.3] under GC3-rpc85-ssp5, per one unit of increase in score.

When examining the relative importance of each context in the joint model using part R-squared (Fig. 4; Supplemental Table 4), the HLT and

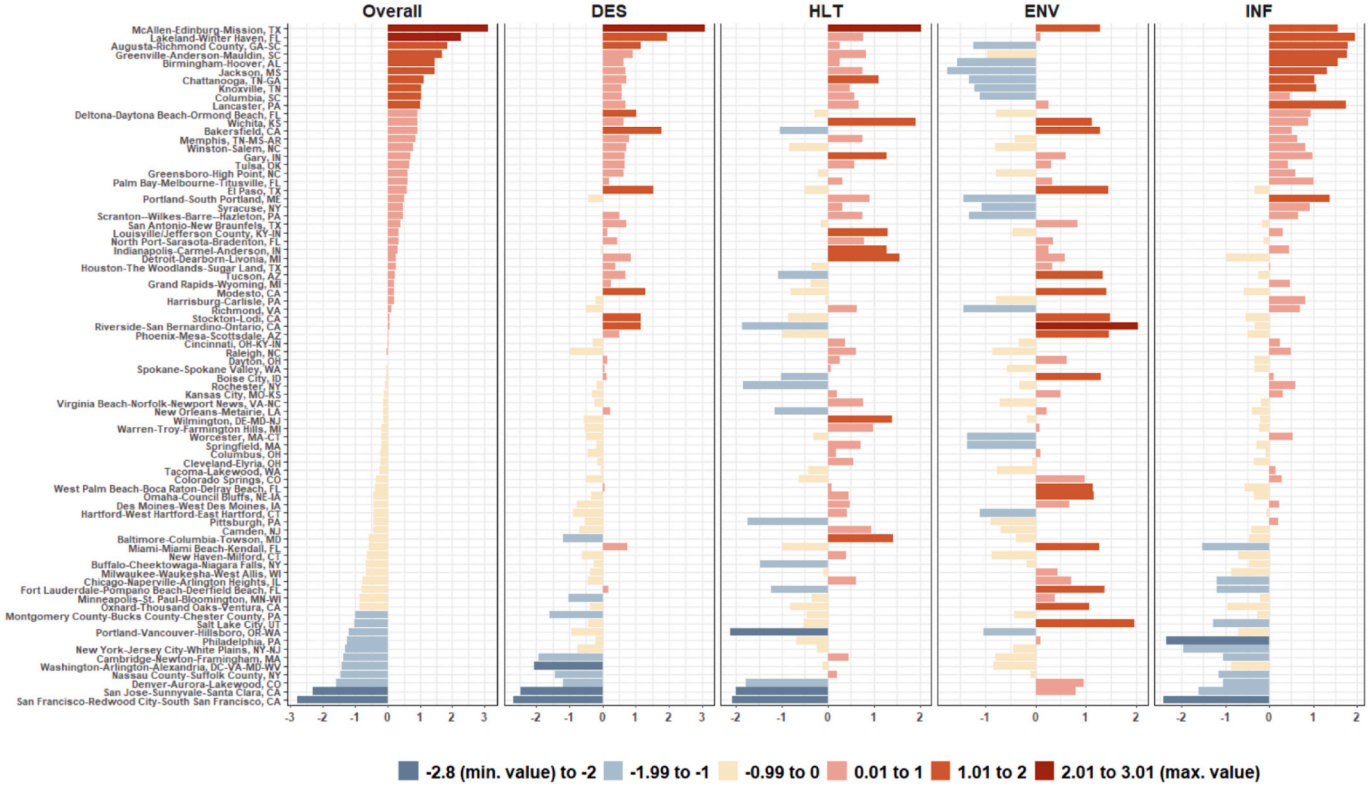

Fig. 3. Urban Heat Health Risk (UHHR) scores, overall and for the demographic and economic status (DES), health (HLT), environment (ENV), and infrastructure (INF) contexts for each of the 80 MSAs for the historical period (2000–2017). Positive values (in warm colors) indicate lower adaptive capacity or increased vulnerability, while negative values (cooler colors) indicate higher adaptive capacity or decreased vulnerability. X-axis represents the UHHR scores, and y-axis represents the 80 MSAs.

Table 3
Associations of overall Urban Heat Health Risk (UHHR) scores and context-specific UHHR scores (demographic and economic status (DES), health (HLT), environment (ENV), and infrastructure (INF)) with the historical period (2000–2017) and change in future excess heat-related cardiovascular disease burden rates. The UHHR scores were generated using confirmatory factor analysis (CFA). Future burden rates are shown for three different scenarios for the near- (2025–2054), mid- (2045–2074), and long-term (2070–2099) and based on CESM-CCSM4 (CC4) under the paired scenarios of Representative Concentration Pathways (RCPs) and Shared Socioeconomic Pathways (SSPs) for moderate emission-middle of the road (rcp45-ssp2) and high emission-fossil fuel development (rcp85-ssp5) and GFDL-CM3 (GC3) under rcp85-ssp5. Results are shown), per unit increase in score. Bold face indicates statistical significance level is < 0.05.

	Overall	DES	HLT	ENV	INF
Historical period	0.55 [-3.16, 4.27]	**5.71 [0.80, 10.62]**	**5.34 [1.49, 9.20]**	−2.45 [-6.91, 2.01]	**−8.81 [-14.27, −3.36]**
CC4-rcp45-ssp2					
Near-term	**2.41 [0.85, 3.96]**	0.37 [-1.84, 2.58]	1.04 [-0.70, 2.78]	1.92 [-0.08, 3.93]	1.97 [-0.48, 4.43]
Mid-term	**4.75 [1.44, 8.07]**	0.29 [-4.37, 4.95]	2.31 [-1.35, 5.97]	**4.89 [0.66, 9.12]**	4.35 [-0.82, 9.52]
Long-term	**9.08 [2.81, 15.35]**	1.48 [-7.35, 10.30]	3.59 [-3.33, 10.51]	**9.04 [1.03, 17.05]**	7.77 [-2.03, 17.56]
CC4-rcp85-ssp5					
Near-term	**4.92 [2.06, 7.79]**	0.51 [-3.53, 4.55]	2.17 [-1.00, 5.35]	**3.93 [0.27, 7.60]**	4.38 [-0.11, 8.86]
Mid-term	**13.57 [4.00, 23.14]**	3.23 [-10.30, 16.76]	4.16 [-6.46, 14.78]	**12.29 [0.01, 24.57]**	11.34 [-3.68, 26.35]
Long-term	**35.14 [3.44, 66.83]**	12.86 [-31.99, 57.71]	7.98 [-27.21, 43.17]	37.53 [-3.17, 78.23]	26.67 [–23.11, 76.44]
GC3-rcp85-ssp5					
Near-term	**7.25 [1.36, 13.15]**	3.18 [-5.13, 11.49]	2.23 [-4.30, 8.75]	7.16 [-0.38, 14.71]	4.57 [-4.66, 13.79]
Mid-term	22.65 [-0.44, 45.73]	10.70 [-21.60, 42.99]	7.18 [-18.17, 32.52]	**30.11 [0.80, 59.42]**	14.36 [-21.48, 50.20]
Long-term	62.11 [-14.65, 138.87]	30.92 [-75.87, 137.70]	17.38 [-66.40, 101.17]	**104.43 [7.52, 201.33]**	42.00 [-76.50, 160.50]

CC4-rcp45-ssp2: Community Climate System Model (CESM-CCSM4) under RCP 4.5 adjusting for population growth for aged 65 and older under SSP2-4.5.
CC4-rcp85-ssp5: Community Climate System Model (CESM-CCSM4) under RCP 8.5 adjusting for population growth for aged 65 and older under SSP5-8.5.
GC3-rcp85-ssp5: Geophysical Fluid Dynamics Laboratory Coupled Model (GCM-CM3) under RCP 8.5 adjusting for population growth for aged 65 and older under SSP5-8.5.

INF scores explained the most variation (6.9 % and 6.4 %, respectively) in health burden at the historical period. Both the HLT and INF scores explained less variances for the future terms, with greater decreases in variances explained by the HLT scores. The variances explained by HLT context decreased to 2.6 % in the near-term under CC4-rcp45-ssp2 and 0.3 % in the long-term under GC3-rcp85-ssp5. In contrast, the role of the ENV context, and to lesser extent the DES context, increased across the near-, mid-, and long-term projections, indicating that the ENV context plays a significant role in future temperature trends and consequently the attributable health burden. Total variances explained by the ENV context changed from 0.7 % at the historical period to 3.5 % in the near-term under CC4-rcp45-ssp2 and 6.8 % in the long-term under GC3-rcp85-ssp5.

3.4. Sensitivity analysis

Sensitivity analysis using the PCA approach showed that the variables selected for each context were generally consistent with those selected by the CFA approach (Supplemental Fig. 1). Though the directions of the factor loadings for the same selected variables in the HLT and INF contexts were opposite to those selected by CFA, the relative magnitudes of the same selected variables in all the contexts were similar. However, the sign of each variable was opposite from its original direction in each individual context when aggregating the selected factors from all the contexts to create overall UHHR scores.

The ranks of the overall UHHR scores created by the PCA approach were mostly consistent with the ranks of scores by the CFA approach but in a reversed direction (Supplemental Fig. 2). The ranges of the scores were much wider (from −10.1 to 8.0) than those created by the CFA approach (from −2.8 to 3.01). The overall UHHR scores from the PCA approach appeared to be dominated by the HLT and INF contexts. MSAs with high HLT and INF often have low DES but inconsistent patterns with the ENV context.

The UHHR scores and xHEAT-CVD burden rates were inversely associated (Supplemental Table 5). One unit increase in overall UHHR scores was consistently associated with decreasing xHEAT-CVD burden rates in the future terms. Negative associations between xHEAT-CVD burden rates and UHHR scores in the HLT context were also apparent for the current and future terms, while positive associations occurred for the ENV context. The associations for the INF context were less conclusive.

When examining the relative importance of each context in the joint model using part R-squared (Supplemental Fig. 3), the HLT and INF scores also explained the most variances of the associations between the UHHR scores and burden at the historical period. Slightly different from the CFA approach, the HLT scores still explained considerable amounts of variances for the future term, whereas INF explained increasingly less, and ENV explained increasingly more of the variances in the associations between xHEAT-CVD burden rates and UHHR scores in all the contexts.

4. Discussion

The health burden of extreme heat is the result of a complex interaction of a wide range of intrinsic and extrinsic factors. With a projected increase in temperature and aging population, it is necessary to identify the drivers of variations in future heat-related health burden. The most influential drivers can then help inform targeted interventions and viable solutions for mitigating the attributable health burden. In this study, we applied IPCC's health risk assessment framework to identify drivers of heat-related cardiovascular morbidity burden across four relevant lived contexts (demographic and economic status, health, environment, and infrastructure) among adults aged 65 and older in 80 US cities. The results of this study suggest several drivers of the future heat-related CVD burden. First, the burden was driven not only by the increase in temperature, but also by the increased number of days with harmful temperatures. Growth in population aged 65 and older also significantly increased the burden. In addition, environmental factors today played an increasingly important role over the time horizons, presumably due to temperature increases and lack of adaptive capacity to mitigate temperature rise. In 2019, the total expenditure related to CVD hospitalizations for the 80 MSAs in this study was around USD$186 billion, according to the Medicare Provider Analysis and Review database (in-house database under the agreement with Center for Medicare & Medicaid Services). Considering that the expenditure for heat-related CVD hospitalizations in US cities is approximately 1.5 % of the total expenditure, as estimated by Cleland et al. (2023), the total expenses are

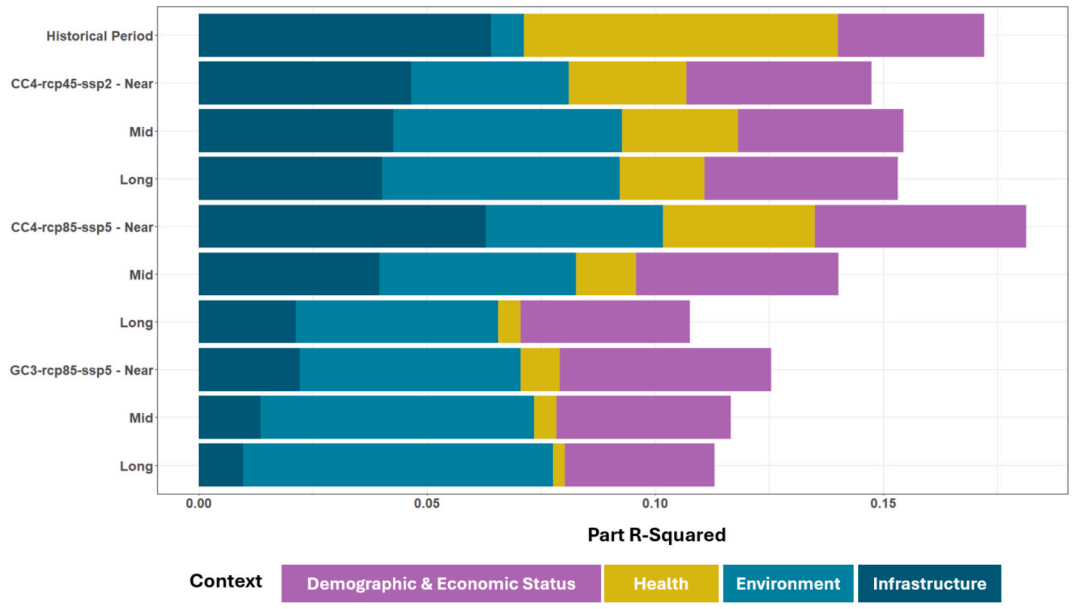

Fig. 4. Part R-squared of demographic and economic status, health, environment, and infrastructure contexts in the joint models explaining the associations with excess heat-related cardiovascular hospitalizations per 100,000 beneficiaries per year (xHEAT-CVD burden rates) for the historical period, and changes in future xHEAT-CVD burden rates under different scenarios and future periods.

estimated to increase by USD$60 billion by the end of the century, after accounting for change in days above MHT and aging population.

Cleland et al. (2023) estimated that the minimum hospitalization percentile was located at the 92nd percentile of the temperature distribution across US MSAs. Here, the temperatures at the minimum hospitalization percentile identified at the historical period were shifted to lower percentiles in future years, indicating that more days will have a temperature exceeding the T_{MHP}, although temperature projections vary substantially based on the GCMs and scenarios (Feng et al., 2014; Tebaldi et al., 2021). These shifts in temperature distributions corresponded to an increase of at least 36 days annually with temperature above T_{MHP} in the long-term under the scenario with the mildest change. This highlights the importance of considering potential intensified effects due to increased durations of periods of high temperature in addition to the increase in temperature itself.

Population growth and structure in the future period were also important. After accounting for population growth rates for those aged 65 and older, which are projected to increase by 2.8 times under SSP2 and by 3.2 times under SSP5 at the mid-term (i.e., 2045–2074), the changes in xHEAT-CVD burden rates are projected to be at least 11.5-fold and 29.0-fold higher than the current burden under those scenarios, respectively. By adjusting for changes in population growth and structure, we address the cautions from previous studies (Cole et al., 2023; de Schrijver et al., 2023) indicating that lack of proper adjustment of changes in population growth and/or structure can underestimate health burden by 50–65 %. Although it is not directly comparable, our findings qualitatively align with Khatana et al. (2024), who reported that the annual excess heat-related mortality rates in the mid-century (i.e., 2036–2065 in their study) among U.S. older adults projected under the higher scenario are about double the projection under the moderate scenario.

This analysis also highlights the importance of environmental factors in shaping future heat-related burden. When examining the relative importance of the DES, HLT, ENV, and INF contexts in explaining the relationships with current and future xHEAT-CVD burden by part R-squared, the HLT and INF contexts explained the most variances in the model for the historical period. Specifically, at historical period, pre-existing health issues (all the selected variables in the HLT context) and access to medical facilities (two of the selected variables in the INF context) were the primary drivers of xHEAT-CVD burden. Across the near-, mid-, and long-term for the future xHEAT-CVD burden, the variances explained by the ENV context gradually increased, and the ENV context gradually replaced most of the variances explained by the HLT and INF contexts at the historical period. The findings that ENV context became the primary driver of the future xHEAT-CVD burden, which were determined by temperature projections, are likely due to the nature that temperature projections are modeled based on environmental characteristics, such as land surface, oceanic, and atmospheric parameters (Danabasoglu et al., 2020; Delworth et al., 2006). Unlike the ENV, INF, and HLT contexts, the variances explained by the DES context remained relatively constant across the historical and future periods. These findings suggest that action plans to alleviate the xHEAT-CVD burden should consider multifaceted approaches with adjustments of focal areas and/or targeting factors that can help tackle multiple issues at different time points or across time. For instance, increased tree cover is associated with heat mitigation (e.g., Ettinger et al., 2024; Wong et al., 2021), reduction in air pollution (e.g., Nowak et al., 2014; Sicard et al., 2025), reduced building energy consumption (e.g., McDonald et al., 2020; Nowak et al., 2017), and improved mental health (e.g., Astell-Burt and Feng, 2019; Callaghan et al., 2021), so investing in tree cover may bring co-benefits for alleviating health burden and improving environments. While addressing the contexts that influence historical xHEAT-CVD burden can help understand the potential causes, developing strategies that can improve the contexts influencing future burden simultaneously may enhance the overall capability to cope and adapt to increasing temperatures.

The heat-health contexts used to characterize adaptive capacity and identify drivers of current and future burden (demographic and economic status, health, environment, and infrastructure) are aligned with the factors reported in previous studies (Li et al., 2022; Niu et al., 2021). Though current indices are built in various spatial scales (e.g., extents, such as one location versus multiple locations, and resolutions, such as gridded, census tract, or county) (Niu et al., 2021), the final sets of factors selected for each context in this study at the MSA scale across the US are generally consistent with previous studies (Cheng et al., 2021; Li et al., 2022).

Moreover, the composite scores of the selected factors in each context indicated that high values of the UHHR scores were indicative of

low adaptive capacity. The characteristics of these high UHHR scores can help planners target areas and approaches to improve adaptive capacity to heat-related health burden. The selected variables in the DES context indicated that MSAs with lower economic resources, lack of social support, and greater economic hardship had higher DES composite scores. For the HLT context, the selected variables indicated that a higher and consistent concentration of individuals with one or more chronic disease resulted in higher HLT composite scores. For the ENV context, MSAs with low canopy, high levels of pollution, less rural canopy, and high frequency of wildfire and drought had higher ENV composite scores. For the INF context, higher INF composite scores were driven by the lack of facilities and transportation network in response to emergency needs. The selection of these factors for the composite scores indicate that they may be valuable to target for heat-health issues at the regional, state, and national levels.

This study has some limitations that are worth noting. Due to limited data availability, this analysis did not include some factors relevant to adaptive capacity, such as prevalence of air conditioning (AC). However, energy burden in summer was used to represent the likelihood of energy consumption by AC usage (De Cian et al., 2025) and the affordability of energy usage in summer. Similarly, due to limited data availability, we were not able to account for physiological (e.g., heat acclimation), behavioral (e.g., changes in physical activity pattern or coping mechanism), infrastructural (e.g., using cooling building materials), institutional (e.g., community preparedness or strategies to heat responses), and medical (e.g., less health issues due to advance in treatments) adaptation. Currently established approaches for estimating future health burden, such as approach taken here, are limited to use the exposure–response function estimated in the historic period across the future periods, while response-exposure function may change over time. Likewise, we were limited to using current and historical observations to explain the relationships with future burden due to the unavailability of future scenarios or trajectories for most factors used in this analysis. Therefore, we advise caution in interpreting the associations between UHHR and future burden reported in this analysis, as they are unlikely to be stationary over time. Additionally, although other climatic factors, such as humidity and wind speed, may play an important role in heat-related health outcomes (Baldwin et al., 2023; Bröde and Kampmann, 2023), we did not use a temperature metric that accounts for these climatic factors, such as Wet Bulb Globe Temperature. However, while the exposure-response function used in this analysis relied solely on daily average temperature as the exposure parameter, it took humidity into account during the modeling process. Future research should also evaluate the xHEAT-CVD burden using metric(s) that take these climatic factors into account. In addition, the temperature projection is not only affected by the global climate models but also the downscaling methods (Manzanas et al., 2018). In this analysis, we used statistical downscaled data, which assumes that the statistical relationships between observed local climatic and large-scale variables stay constant over time (i.e., stationarity assumption) (Wang et al., 2018). However, it is unlikely that the relationships observed in the historical period will remain the same in the future. Though previous research reports that temperature projections from statistically and dynamically downscaled data tend to agree with each other (Murphy, 1999; Pierce et al., 2013; Sparks et al., 2017), future research should still consider evaluating the heat-health risks using data from both downscaling techniques to have a more comprehensive understanding on the future heat-health burden. Lastly, this analysis was only conducted for urban areas with a focus on older adults. Although older individuals have been identified as one of the most high-risk groups to heat impacts and are well-represented in the Medicare program, with an estimation of 94 % of the individuals older than 65 enrolled in the program (Lindstrom et al., 2024), it is also important to understand the risks among other populations. However, focusing on one large risk group at the time can be beneficial from program implementation perspective because the information can better integrate with the established channels of communication and access to information which are often unique to group. For example, number of organizations and medical professional groups who specialize in care for older individuals are keenly aware of how, when, and where specific population (e.g., Medicare beneficiaries) receive information and resources. Similarly, there are number of organizations that focus on children and individuals with chronic diseases which are also susceptible to health impacts of temperature. Additionally, heat-health burden in rural areas is increasing (Cross et al., 2021) and it is important to identify the factors and key areas for mitigating heat-health burden in rural areas. Future research is needed for a more comprehensive understanding of the drivers of heat-health risks and burdens across various landscapes and populations, since other populations may not share similar pathways of exposure and effects as the older individuals.

Notwithstanding, this study has several strengths that make significant contributions to the existing literature. First, we estimated the xHEAT-CVD burden at multiple timeframes across the US, which provides a more comprehensive understanding of the impacts of excess heat on CVD burden and the differing intensity of change in burden over time. Though previous research has assessed future CVD burden across the US (e.g., Khatana et al., 2024; Mohebi et al., 2022), to our knowledge our study is the first to estimate xHEAT-CVD burden among US older adults for multiple future terms. Second, among the existing indices addressing heat and health issues, only a small number of studies conducted validation processes to evaluate the efficacy of indices through examining the correlations and/or associations with present-day health burden (Cheng et al., 2021; Li et al., 2022). This study validated the UHHR scores with not only present-day but also future CVD burden. In addition, the validation was conducted for the overall UHHR score, as well as by the context-specific scores. Third, most existing studies developed indices using only one method (Cheng et al., 2021; Li et al., 2022). In contrast, we created the UHHR scores primarily using CFA but also employed the most used method, PCA, for comparison. The findings in this study indicate that the "most" appropriate methods for creating indice(s) may depend on study purposes and designs.

5. Conclusions

There are increasing efforts to assess heat-related health issues from different perspectives across the world. This study estimates the impacts of future CVD burden due to excess heat in US metropolitan areas and develops a urban heat health risk score that captures four distinct contexts relevant to adaptive capacity. These contexts were defined using factors that were shown to be significantly associated with current and future heat-related CVD burden. Findings from this study not only provide additional contributions to the existing literature on the potential drivers of heat-health burden but also identify additional areas of focus for mitigating the heat-health burden at different forward-looking timeframes. To mitigate the potential increase in future heat-related CVD burden, action plans are encouraged to use multifaceted approaches that address the different drivers of vulnerability and adaptive capacity.

CRediT authorship contribution statement

Wei-Lun Tsai: Writing – review & editing, Writing – original draft, Visualization, Validation, Project administration, Methodology, Investigation, Formal analysis, Data curation, Conceptualization. **E.Melissa Mcinroe:** Writing – review & editing, Formal analysis, Data curation. **Anna M. Jalowska:** Writing – review & editing, Writing – original draft, Methodology, Data curation. **Corinna Y. Keeler:** Writing – review & editing, Writing – original draft, Methodology, Conceptualization. **Stephanie E. Cleland:** Writing – review & editing, Methodology, Conceptualization. **Cassandra R. O'Lenick:** Writing – review & editing, Methodology, Data curation, Conceptualization. **Tanya L. Spero:** Writing – review & editing, Methodology, Data curation. **Alexandra Schneider:** Writing – review & editing, Methodology,

Conceptualization. **Ana G. Rappold:** Writing – review & editing, Writing – original draft, Supervision, Methodology, Investigation, Conceptualization.

Declaration of competing interest

The authors declare that they have no known competing financial interests or personal relationships that could have appeared to influence the work reported in this paper.

Acknowledgements

The authors would like to thank Drs. Haiyan Tong and Neal Fann for their time and thoughtfulness in providing valuable feedback. We would also like to thank our former colleagues, Drs. Mallory Turner and Lucas Neas and Mr. K. Lloyd Hill, for their efforts in establishing foundational work for this analysis. The views expressed in this article are those of the authors and do not necessarily reflect the views or policies of the U.S. Environmental Protection Agency.

Disclaimer: The research described in this article has been reviewed by the Center for Environmental Public Health and Environmental Assessment, U.S. Environmental Protection Agency and approved for publication. The contents of this article should not be construed to represent agency policy, nor does mention of trade names or commercial products constitute endorsement or recommendation for use.

Appendix A. Supplementary data

Supplementary data to this article can be found online at https://doi.org/10.1016/j.envint.2025.110022.

Data availability

Data will be made available on request.

References

Astell-Burt, T., Feng, X., 2019. Association of urban green space with mental health and general health among adults in Australia. JAMA Netw. Open 2, e198209–e.
Azhar, G., et al., 2017. Heat wave vulnerability mapping for India. Int. J. Environ. Res. Public Health 14, 357.
Baldwin, J.W., et al., 2023. Humidity's role in heat-related health outcomes: a heated debate. Environ. Health Perspect. 131, 055001.
Bröde, P., Kampmann, B., 2023. Temperature–humidity-dependent wind effects on physiological heat strain of moderately exercising individuals reproduced by the universal thermal climate index (UTCI). Biology 12, 802.
Callaghan, A., et al., 2021. The impact of green spaces on mental health in urban settings: a scoping review. J. Ment. Health 30, 179–193.
Chen, K., et al., 2024. Impact of population aging on future temperature-related mortality at different global warming levels. Nat. Commun. 15, 1796.
Cheng, W., et al., 2021. Approaches for identifying heat-vulnerable populations and locations: a systematic review. Sci. Total Environ. 799, 149417.
Cleland, S.E., et al., 2023. Urban heat island impacts on heat-related cardiovascular morbidity: a time series analysis of older adults in US metropolitan areas. Environ. Int. 178, 108005.
Cole, R., et al., 2023. The contribution of demographic changes to future heat-related health burdens under climate change scenarios. Environ. Int. 173, 107836.
Conlon, K.C., et al., 2020. Mapping human vulnerability to extreme heat: a critical assessment of heat vulnerability indices created using principal components analysis. Environ. Health Perspect. 128, 097001.
Cross, S.H., et al., 2021. Rural-urban disparity in mortality in the US from 1999 to 2019. J. Am. Med. Assoc. 325, 2312–2314.
Cutter, S.L., et al., 2003. Social vulnerability to environmental hazards. Soc. Sci. Q. 84, 242–261.
Danabasoglu, G., et al., 2020. The Community Earth System Model version 2 (CESM2). J. Adv. Model. Earth Syst. 12, e2019MS001916.
De Cian, E., et al., 2025. The impact of air conditioning on residential electricity consumption across world countries. J. Environ. Econ. Manag. 131, 103122.
de Schrijver, E., et al., 2023. Exploring vulnerability to heat and cold across urban and rural populations in Switzerland. Environ. Res.: Health 1, 025003.
Delworth, T.L., et al., 2006. GFDL's CM2 global coupled climate models. Part I: Formulation and simulation characteristics. J. Clim. 19, 643–674.
Donner, L.J., et al., 2001. The dynamic core, physical parameterizations, and basic simulation characteristics of the atmospheric component AM3 of the GFDL Global coupled Model CM3. J. Clim. 24, 3484–3519.
Ebi, K.L., et al., 2021. Hot weather and heat extremes: Health risks. Lancet 398, 698–708.
Ellena, M., et al., 2020. The heat-health nexus in the urban context: a systematic literature review exploring the socio-economic vulnerabilities and built environment characteristics. Urban Clim. 34, 100676.
Estoque, R.C., et al., 2023. Has the IPCC's revised vulnerability concept been well adopted? Ambio 52, 376–389.
Ettinger, A.K., et al., 2024. Street trees provide an opportunity to mitigate urban heat and reduce risk of high heat exposure. Sci. Rep. 14, 3266.
Feng, S., et al., 2014. Projected climate regime shift under future global warming from multi-model, multi-scenario CMIP5 simulations. Global Planet. Change 112, 41–52.
García-León, D., et al., 2024. Temperature-related mortality burden and projected change in 1368 European regions: a modelling study. Lancet Public Health 9, e644–e653.
Gent, P.R., et al., 2011. The Community climate System Model version 4. J. Clim. 24, 4973–4991.
Gronlund, C.J., 2014. Racial and socioeconomic disparities in heat-related health effects and their mechanisms: a review. Curr. Epidemiol. Rep. 1, 165–173.
Gronlund, C.J., et al., 2015. Vulnerability to extreme heat by socio-demographic characteristics and area green space among the elderly in Michigan, 1990-2007. Environ. Res. 136, 449–461.
Harlan, S.L., et al., 2006. Neighborhood microclimates and vulnerability to heat stress. Soc. Sci. Med. 63, 2847–2863.
Hauer, Center for International Earth Science Information Network (CIESIN) at Columbia University, Georeferenced U.S. County-level population projections, total and by sex, race and age, based on the SSPs, 2020-2100. Palisades, NY: NASA socioeconomic data and applications center (SEDAC). 10.7927/dv72-s254. Accessed on 21 January 2025.
Hijmans, R. J., 2018. Raster: Geographic data analysis and modeling. R package version. 2, 8.
Ho, H.C., et al., 2015. A spatial framework to map heat health risks at multiple scales. Int. J. Environ. Res. Public Health 12, 16110–16123.
IPCC, Summary for policymakers. In: T. F. Stocker, et al., (Eds.), In: Climate Change 2013: The Physical Science Basis. Contribution of Working Group I to the Fifth Assessment Report of the Intergovernmental Panel on Climate Change, Vol. 3. Cambridge University Press Cambridge, United Kingdom and New York, NY, USA, 2013, pp. 159-204.
IPCC, 2023. Intergovernmental Panel on Climate Change. IPCC Sixth Assessment Report (AR6) synthesis report: Climate change 2023. Intergovernmental Panel on Climate Change.
Jalowska, A.M., et al., 2025. Assessing flooding from changes in extreme rainfall: using the Design Rainfall Approach in hydrologic modeling. Water 17, 2228.
Johnson, D.P., et al., 2012. Developing an applied extreme heat vulnerability index utilizing socioeconomic and environmental data. Appl. Geogr. 35, 23–31.
Kalisa, E., et al., 2018. Temperature and air pollution relationship during heatwaves in Birmingham, UK. Sustain. Cit. Soc. 43, 111–120.
Khatana, S.A.M., et al., 2024. Projections of extreme temperature–related deaths in the US. JAMA Netw. Open 7, e2434942.
Lee, J.-Y., et al., 2021. Future global climate: Scenario-based projections and nearterm information. In climate change 2021: The physical science basis. Contribution of working group i to the sixth assessment report of the intergovernmental panel on climate change [Masson-Delmotte, V., et al. (eds.)]. Cambridge University Press, Cambridge, United Kingdom and New York, NY, USA. 553-672.
Li, F., et al., 2022. Understanding urban heat vulnerability assessment methods: a PRISMA review. Energies 15, 6998.
Lin, S., et al., 2009. Extreme high temperatures and hospital admissions for respiratory and cardiovascular diseases. Epidemiology 20, 738–746.
Lindstrom, R. et al., 2024. Percentage of older adults with both private health insurance and medicare decreased from 2017 to 2022. Us census bureau. https://www.Census.Gov/library/stories/2024/04/older-adults-health-coverage.html.
Liu, J., et al., 2022. Heat exposure and cardiovascular health outcomes: a systematic review and meta-analysis. Lancet Planet. Health. 6, e484–e495.
Madrigano, J., et al., 2015. Temperature, ozone, and mortality in urban and non-urban counties in the northeastern United States. Environ. Health 14, 3.
Manzanas, R., et al., 2018. Dynamical and statistical downscaling of seasonal temperature forecasts in Europe: added value for user applications. Clim. Serv. 9, 44–56.
Maragno, D., et al., 2020. Mapping heat stress vulnerability and risk assessment at the neighborhood scale to drive urban adaptation planning. Sustainability 12, 1056.
McDonald, R.I., et al., 2020. The value of US urban tree cover for reducing heat-related health impacts and electricity consumption. Ecosystems 23, 137–150.
Moghadamnia, M.T., et al., 2017. Ambient temperature and cardiovascular mortality: a systematic review and meta-analysis. PeerJ 5, e3574.
Mohebi, R., et al., 2022. Cardiovascular disease projections in the United States based on the 2020 census estimates. JACC 80, 565–578.
Murphy, J., 1999. An evaluation of statistical and dynamical techniques for downscaling local climate. J. Clim. 12, 2256–2284.
Naughton, M.P., et al., 2002. Heat-related mortality during a 1999 heat wave in Chicago. Am. J. Prev. Med. 22, 221–227.
Nayak, S.G., et al., 2018. Development of a heat vulnerability index for New York state. Public Health 161, 127–137.
Niu, Y., et al., 2021. A systematic review of the development and validation of the heat vulnerability index: Major factors, methods, and spatial units. Curr. Climate Change Rep. 7, 87–97.
Nolte, C., et al., 2018. Air quality. Impacts, risks, and adaptation in the United States: Fourth National Climate Assessment. 2, 512-538.

Nolte, C.G., et al., 2021. Regional temperature-ozone relationships across the US under multiple climate and emissions scenarios. J. Air Waste Manage. Assoc. 71, 1251–1264.
Nowak, D.J., et al., 2017. Residential building energy conservation and avoided power plant emissions by urban and community trees in the United States. Urban For. Urban Green. 21, 158–165.
Nowak, D.J., et al., 2014. Tree and forest effects on air quality and human health in the United States. Environ. Pollut. 193, 119–129.
O'Lenick, C. R., et al., 2019. Urban heat and air pollution: A framework for integrating population vulnerability and indoor exposure in health risk analyses. The Science of the total environment. 660.
O'Neill, B.C., et al., 2014. A new scenario framework for climate change research: the concept of shared socioeconomic pathways. Clim. Change 122, 387–400.
Phung, D., et al., 2016. Ambient temperature and risk of cardiovascular hospitalization: an updated systematic review and meta-analysis. Sci. Total Environ. 550, 1084–1102.
Pierce, D., LOCA statistical downscaling (localized constructed analogs). 2021.
Pierce, D.W., et al., 2014. Statistical downscaling using localized constructed analogs (LOCA). J. Hydrometeorol. 15, 2558–2585.
Pierce, D.W., et al., 2013. Probabilistic estimates of future changes in California temperature and precipitation using statistical and dynamical downscaling. Clim. Dyn. 40, 839–856.
Reid, C.E., et al., 2009. Mapping community determinants of heat vulnerability. Environ. Health Perspect. 117, 1730–1736.
Rohat, G., et al., 2019. Influence of changes in socioeconomic and climatic conditions on future heat-related health challenges in Europe. Global Planet. Change 172, 45–59.
Rosseel, Y., 2012. Lavaan: an R package for structural equation modeling. J. Stat. Softw. 48, 1–36.
Sanderson, B.M., et al., 2017. Skill and independence weighting for multi-model assessments. Geosci. Model Dev. 10, 2379–2395.
Sheffield, J., et al., 2013. North American climate in CMIP5 experiments. Part I: Evaluation of historical simulations of continental and regional climatology. J. Clim. 26, 9209–9245.
Shen, Z., et al., 2023. Community vulnerability is the key determinant of diverse energy burdens in the United States. Energy Res. Soc. Sci. 97, 102949.
Sicard, P., et al., 2025. Effect of tree canopy cover on air pollution-related mortality in European cities: an integrated approach. Lancet Planet. Health. 9, e527–e537.
Sparks, M.M., et al., 2017. Thermal adaptation and phenotypic plasticity in a warming world: Insights from common garden experiments on Alaskan sockeye salmon. Glob. Chang. Biol. 23, 5203–5217.
Spero, T.L., et al., 2016. The impact of incongruous lake temperatures on regional climate extremes downscaled from the CMIP5 archive using the WRF model. J. Clim. 29, 839–853.
Tebaldi, C., et al., 2021. Climate model projections from the scenario model intercomparison project (ScenarioMIP) of CMIP6. Earth Syst. Dyn. 12, 253–293.
Tobías, A., et al., 2017. Brief report: investigating uncertainty in the minimum mortality temperature: Methods and application to 52 Spanish cities. Epidemiology 28, 72–76.
U.S. Census Bureau, County population totals: 2010-2019. Available at https://www.Census.Gov/data/tables/time-series/demo/popest/2010s-counties-total.Html. Accessed on 12 May, 2020. 2020.
United Nations Statistics Division, 2025. Population by age, sex, and urban/rural residence. UN Data. Available at https://data.un.org/Default.aspx. Accessed on June 17, 2025.
USGS Geo Data Portal, Available at https://www.Usgs.Gov/tools/geo-data-portal. Accessed on October 12, 2023. 2023.
van Vuuren, D.P., et al., 2011. The representative concentration pathways: an overview. Clim. Change 109, 5.
Vandentorren, S., et al., 2006. August 2003 heat wave in France: risk factors for death of elderly people living at home. Eur. J. Pub. Health 16, 583–591.
Wang, Y., et al., 2018. The stationarity of two statistical downscaling methods for precipitation under different choices of cross-validation periods. Int. J. Climatol. 38, e330–e348.
Wilhelmi, O.V., Hayden, M.H., 2010. Connecting people and place: a new framework for reducing urban vulnerability to extreme heat. Environ. Res. Lett. 5, 014021.
Wong, N.H., et al., 2021. Greenery as a mitigation and adaptation strategy to urban heat. Nat. Rev. Earth Environ. 2, 166–181.
Zhao, Q., et al., 2021. Global, regional, and national burden of mortality associated with non-optimal ambient temperatures from 2000 to 2019: a three-stage modelling study. Lancet Planet. Health. 5, e415–e425.